

Geodesic congruences in warped spacetimes

Suman Ghosh ^{1*}, Anirvan Dasgupta ^{2,3 †} and Sayan Kar^{1,3 ‡}

¹*Department of Physics and Meteorology,*

Indian Institute of Technology,

Kharagpur 721 302, India

²*Department of Mechanical Engineering,*

Indian Institute of Technology,

Kharagpur 721 302, India

³*Centre for Theoretical Studies,*

Indian Institute of Technology,

Kharagpur 721 302, India

* E-mail:suman@cts.iitkgp.ernet.in

† E-mail:anir@cts.iitkgp.ernet.in

‡ E-mail:sayan@cts.iitkgp.ernet.in

Abstract

In this article, we explore the kinematics of timelike geodesic congruences in warped five dimensional bulk spacetimes, with and without thick or thin branes. We begin our investigations with the simplest case, namely geodesic flows in the Randall–Sundrum AdS (Anti de Sitter) geometry without and with branes. Analytical expressions for the expansion scalar are obtained and the effect of including one or more thin branes (i.e. a background which is a slice of AdS spacetime) on its evolution, is pointed out. Subsequently, we move on to studying such congruences in more general warped bulk geometries with a cosmological thick brane and a time-dependent extra dimensional scale. Using the analytical expressions for the velocity field components, we interpret the expansion, shear and rotation (ESR) along the flows. The evolution of a cross-sectional area orthogonal to the congruence, as seen from a local observer’s point of view, is also shown graphically. Finally, the Raychaudhuri and geodesic equations in the backgrounds with a thick brane are solved numerically in order to figure out the role of initial conditions (prescribed on the ESR) and space-time curvature on the evolution of the ESR. Apart from other aspects seen, we specially note the effect of increasing the initial rotation on the delay in appearance of a congruence singularity. This feature is also illustrated through the evolution of a cross sectional area. Our results characterise specific features of timelike geodesic flows which can arise due to warping, the presence/absence of a brane, a cosmological line element and/or a time-dependent extra dimensional scale.

Keywords: Geodesic congruence, Raychaudhuri equation, extra dimension, braneworld.

PACS numbers: 04.50.+h, 12.10.-g

I. INTRODUCTION

Almost a century ago, in their pioneering research [1], Kaluza and Klein (KK) proposed unification of four dimensional gravity and electromagnetism in a five dimensional gravity framework. This proposal raised a fair amount of curiosity, interest and research activity among theoretical physicists on the physics of extra dimensions. The idea of extra spatial dimensions appeared in a new incarnation with the advent of Superstring theories [2]. The theoretical existence of branes in String theory eventually motivated the hypothesis that we may be living on an embedded, timelike submanifold (the brane) of a higher dimensional ($D > 4$) Lorentzian spacetime (warped or unwarped), as assumed in the so-called Arkani-Hamed–Dvali–Dimopoulos (ADD) [3] and Randall–Sundrum (RS) [4] braneworld models.

The original work of Randall and Sundrum (RS) [4, 5] on warped braneworlds, published a decade ago, refers to the idea of the scale of the extra dimension being spacetime dependent, while addressing the issue of stability, in a two-brane scenario. In a single brane scenario or from a purely higher dimensional bulk perspective, the space-time dependence of the metric function(s) associated with the extra dimensional coordinate(s) basically imply that the scale of the extra dimension depends on the on-brane or four dimensional spacetime coordinates. To visualise this, it is easiest to go back to the early Kaluza-Klein (KK) universe models with different scale factors associated with the evolution of each set of non-compact/compact dimensions (usual or extra). The difference between today’s warped braneworlds and the KK idea, is the warped geometry and also the non-compact extra dimension(s). We shall be mostly concerned with the single brane scenario and a five dimensional bulk, in this article.

In an earlier paper [6], geodesics in warped spacetimes have been investigated in detail. However, such a study of geodesics alone cannot tell us about the overall local behavior of a family of test particles as observed in the neighbourhood of a freely falling observer. This motivates us to study the evolution of geodesic congruences. Ever since the appearance of *Raychaudhuri equations*, in 1955 [7], relativists have discussed and analysed its implications in various contexts. In its original incarnation, the Raychaudhuri equations provided the basis for the description and analysis of spacetime singularities in gravitation and cosmology [8]. For example, the equation for the expansion and the resulting theorem on geodesic focusing, is a crucial ingredient in the proofs of Penrose-Hawking singularity theorems [9, 10].

The kinematics of geodesic congruences is characterised by three kinematical quantities:

isotropic expansion, shear and rotation (henceforth referred as ESR) [11–16], which evolve along the flow according to the Raychaudhuri equations. Though mostly quoted and used in the context of gravity, these equations by virtue of their geometric nature, have a much wider scope in studying geodesic as well as non-geodesic flows in nature, which may possibly arise in diverse contexts (see [16] for some open issues). Two of the authors here have recently used these equations to investigate the kinematics of geodesic flows in stringy black hole spacetimes [17] and flows on flat and curved deformable media (including elastic and viscoelastic media) in detail [18, 19].

In this article, we attempt to understand the kinematics of geodesic flows in five dimensional warped bulk spacetimes with and without branes. We begin with a study of the kinematics of geodesic congruences in the simplest bulk—the Randall–Sundrum AdS (Anti de Sitter) spacetime with and without branes. Thereafter, we move on to investigations on geodesic flows in warped bulk spacetimes with a cosmological thick brane and a time-dependent extra dimension. We first obtain the ESR using the geodesic velocity field expressions. The evolution of a cross-sectional area orthogonal to the flow, as seen from a local observer’s frame is also presented. Subsequently, we obtain u^A as well as the ESR, numerically, by imposing initial conditions on them, and evolving the full system of equations (geodesic and Raychaudhuri) along the flow. This approach (primarily numerical) enables us to obtain the tangent vector field as well as the ESR simultaneously and highlights the role of the initial conditions on all variables. In order to facilitate visualisation, we show the evolution of a cross-sectional area here, as well. Our main motivation behind the work reported here, is to find how the evolution of the ESR are affected by the presence of various metric functions that characterise and distinguish different five dimensional bulk spacetimes with and without thin and thick branes.

Let us assume a bulk line element of the form,

$$ds^2 = e^{2f(\sigma)} [-dt^2 + a^2(t) d\mathbf{X}^2] + b^2(t) d\sigma^2, \quad (1.1)$$

where $d\mathbf{X}^2 = dx^2 + dy^2 + dz^2$. Here, the function $b(t)$ represents the scale of the extra dimension while the $a(t)$ and $e^{2f(\sigma)}$ are the usual cosmological scale and warp factors, respectively. We intend to delineate how the features of ESR change when we vary the nature of each of the three functions $a(t)$, $b(t)$ and $f(\sigma)$. The geodesic equations cannot be solved analytically (modulo a few simplistic cases) in a spacetime as complicated as represented

by (1.1). However, first integrals can be found and the ESR may be obtained analytically. For the numerical analysis of the system of differential equations, as detailed in the previous paragraph, we have used standard numerical codes.

Our article is organised as follows. We first review the background spacetime geometry and discuss our choices for the various metric functions (Section II). Section III reviews the geodesics following our earlier work [6]. In Section IV, we first state the definitions of the ESR and write down the evolution (Raychaudhuri) equations for geodesic flows in such a background metric. Further, in Section IV-A, we discuss geodesic flows in the Randall Sundrum AdS spacetime with and without branes. Section IV-B contains the ESR as found from the definitions, using the velocity field. Here we also discuss the evolution of the cross-sectional area orthogonal to the flow. The numerical analysis of the Raychaudhuri and geodesic equations as an initial value problem is presented in Section IV-C. Finally, in Section V, we summarise our results and conclude with a few remarks.

II. THE BACKGROUND SPACETIME GEOMETRIES

We consider the metric given by equation (1.1) rewritten using conformal time (η), as follows,

$$ds^2 = e^{2f(\sigma)} a^2(\eta) [-d\eta^2 + d\mathbf{X}^2] + b^2(\eta) d\sigma^2. \quad (2.1)$$

To arrive at concrete results in the following Sections, we need to choose the functional forms of the warp factor as well as the cosmological and extra dimensional scale factors. For the warp factor e^{2f} we choose,

$$f(\sigma) = \begin{cases} -\ln(\cosh k\sigma) & \rightarrow \text{represents a decaying warp factor,} \\ \ln(\cosh k\sigma) & \rightarrow \text{represents a growing warp factor,} \end{cases} \quad (2.2)$$

which correspond to the well-known thick brane models [20–22]. In such models, the brane is dynamically generated as a scalar field domain wall (soliton) in the bulk. Note that the warp factor in such models is a smooth function of the extra dimension, unlike the RS case where we have $f(\sigma) = -k|\sigma|$ (i.e. a function with a derivative jump which implies thin branes in the bulk, realised via delta functions in the stress energy). We choose to work with thick branes mainly to avoid the jumps and delta functions which will appear in the connection and curvature for thin branes. However, as we will see later, in some special

cases (e.g. Einstein spaces) one can indeed solve the Raychaudhuri equations consistently, with zero rotation and shear, in the presence of thin branes.

What do we choose for the scale factors? Two different combinations of $a(\eta)$ and $b(\eta)$, chosen as models to represent different kinds of time evolution, are given below in terms of the cosmological time “ t ”,

$$\{a(t), b(t)\} = (i) \{a_0 t^{\nu_1}, b_0 + b_1 t^{-\nu_2}\}, \quad \text{and} \quad (ii) \{a'_0 e^{H(t-t_0)}, b'_0 + b'_1 e^{-\beta H(t-t_0)}\}, \quad (2.3)$$

where we take ν_1 to span over an open interval $(0, 1)$, so that in (i) $a(t)$ represents an expanding but decelerating on-brane line element (which is radiative for $\nu_1 = \frac{1}{2}$), and in (ii) we take H to be positive, representing an accelerating de-Sitter on-brane line element. $b_0, b_1, \nu_2, b'_0, b'_1$ and β are positive so that we have a decaying extra dimension which stabilizes to a finite value as $t \rightarrow \infty$. The type of metric functions we consider here may be obtained as analytic solutions of the five dimensional Einstein equations with the corresponding Einstein tensors providing matter energy-momentum profiles through the Einstein field equations. As shown in [23], for similar metric functions, the corresponding matter stress-energy can indeed satisfy the Weak Energy Condition. It may be noted that these models are assumed to represent the evolution of the universe beginning at a finite time $t = t_0 (\neq 0)$ when both the scales of visible and extra dimension were same.

Using conformal time, the scale factors in set (i) and set (ii) can be re-expressed as [6]

$$a(\eta) = \frac{t_0}{1 - \nu_1} \eta^{\frac{\nu_1}{1 - \nu_1}}, \quad b(\eta) = t_0 \left(\frac{\nu_1}{1 - \nu_1} + \eta^{\frac{-\nu_2}{1 - \nu_1}} \right), \quad 1 \leq \eta \leq \infty \quad (2.4)$$

and

$$a(\eta) = \frac{1}{H} \frac{1}{(1 - \eta)} \quad b(\eta) = \frac{1}{H} \left[1 - b'_1 H \{1 - (1 - \eta)^\beta\} \right], \quad 0 \leq \eta \leq 1 \quad (2.5)$$

respectively. As a specific case, let us consider, $\nu_1 = \nu_2 = \frac{1}{2}$, $t_0 = 1$, $H = 1$, $b'_1 = \frac{1}{2}$ and $\beta = 1$ which leads to the following two different combinations of the scale factors,

$$\begin{aligned} \text{(A)} \quad & a(\eta) = 2\eta, \quad b(\eta) = 1 + \frac{1}{\eta}, \\ \text{(B)} \quad & a(\eta) = \frac{1}{1 - \eta}, \quad b(\eta) = 1 - \frac{\eta}{2}. \end{aligned}$$

These combinations of scale factors will henceforth be abbreviated as Set(A) and Set(B).

III. GEODESICS

The general form of the constraint (i.e. $g_{AB}u^A u^B = -\epsilon$) for null and timelike geodesics corresponding to the metric (2.1) is given below,

$$e^{2f(\sigma)} a^2(\eta) [-\dot{\eta}^2 + \dot{\mathbf{X}}^2] + b(\eta)^2 \dot{\sigma}^2 + \epsilon = 0, \quad (3.1)$$

where $\epsilon = 1$ and 0 denote the cases corresponding to the timelike and null geodesics, respectively, and, a dot here represents differentiation with respect to the affine parameter λ . As x_i is cyclic for the geodesics corresponding to 2.1, we have

$$\dot{x}_i = \frac{C_i e^{-2f}}{a^2}, \quad (3.2)$$

where C_i 's are integration constants. The full geodesic equations

$$\frac{d^2 x^A}{d\lambda^2} + \Gamma_{CD}^A \frac{dx^C}{d\lambda} \frac{dx^D}{d\lambda} = 0 \quad (3.3)$$

in a spacetime corresponding to the metric (2.1) are very difficult to solve analytically. However, Eq.3.3 can be recast as the following first order dynamical system of coupled differential equations [6],

$$\dot{\eta} = \frac{e^{-f(\sigma)}}{a(\eta)} \sqrt{\epsilon + \frac{\sum_{i=1}^3 C_i^2}{e^{2f(\sigma)} a^2(\eta)} + \frac{\chi^2}{b^2(\eta)}}, \quad (3.4)$$

$$\dot{x}_i = \frac{C_i e^{-2f(\sigma)}}{a^2(\eta)}, \quad (3.5)$$

$$\dot{\sigma} = \frac{\chi}{b^2(\eta)}, \quad (3.6)$$

$$\text{and } \dot{\chi} = -f'(\sigma) \left(\epsilon + \frac{\chi^2}{b^2(\eta)} \right). \quad (3.7)$$

by defining a new quantity $\chi(\lambda)$ given by Eq.3.6. Here the dots represent differentiation with respect to the affine parameter λ , while primes denote differentiation of the respective functions, with respect to their corresponding independent variables, η or σ . Thus, for simple cases, one can find the first integrals of the geodesic equations directly from the above relations and these can be then be used to determine the ESR.

IV. RAYCHAUDHURI EQUATION AND ESR VARIABLES

To quantify the different kinematical quantities that characterize the flow of a geodesic congruence (family of non-intersecting integral curves generated by a given geodesic vector

field) in a given background spacetime, the gradient of the velocity field is split into following three parts,

$$\nabla_B u_A = \Sigma_{AB} + \Omega_{AB} + \frac{1}{n-1} h_{AB} \Theta, \quad (4.1)$$

where, n is the dimension of spacetime and $h_{AB} = g_{AB} \pm u_A u_B$ is the projection tensor (the plus sign is for timelike curves whereas the minus one is for spacelike ones) and $u_A u^A = \mp 1$. Θ , the trace of $\nabla_B u_A$, represents the isotropic expansion, Σ_{AB} is the symmetric, traceless part representing the shear and Ω_{AB} are the components of the antisymmetric rotation tensor. Therefore, by definition

$$\Theta = \nabla_A u^A, \quad (4.2)$$

$$\Sigma_{AB} = \frac{1}{2} (\nabla_B u_A + \nabla_A u_B) - \frac{1}{n-1} h_{AB} \Theta, \quad (4.3)$$

$$\Omega_{AB} = \frac{1}{2} (\nabla_B u_A - \nabla_A u_B). \quad (4.4)$$

It is interesting to note that for geodesic congruences with zero rotation, one can always write $u_A = \partial_A \Phi$, where $\Phi(x^A)$ is a scalar function. Thus, the expansion scalar can be redefined as $\Theta = \square \Phi$. One can find this scalar function by integrating the velocity vector field. One such example is shown later.

We now turn towards writing down the evolution equations for the expansion, shear and rotation along the flow, representing a timelike geodesic congruence. A fact worth mentioning here is that, these evolution equations (and their generalisations) are essentially *geometric statements* and are independent of any reference to the Einstein field equations.

The modern (textbook) way to derive these equations (see [12]) is as follows. Consider the quantity $u^C \nabla_C B_{AB}$ (where $B_{AB} = \nabla_B u_A$). Evaluating this as an identity we get

$$u^C \nabla_C B_{AB} = -B_{AC} B_B^C - R_{ACBD} u^C u^D. \quad (4.5)$$

Then splitting the above equation into its trace, symmetric traceless and anti-symmetric parts, we have

$$\frac{d\Theta}{d\lambda} + \frac{1}{n-1} \Theta^2 + \Sigma^2 - \Omega^2 = -R_{AB} u^A u^B \quad (4.6)$$

$$\begin{aligned} u^C \nabla_C \Sigma_{AB} = & -\frac{2}{n-1} \Theta \Sigma_{AB} - \Sigma_{AC} \Sigma_B^C - \Omega_{AC} \Omega_B^C + \frac{1}{n-1} h_{AB} (\Sigma^2 - \Omega^2) \\ & + W_{CBAD} u^C u^D + \frac{1}{n-2} \tilde{R}_{AB} \end{aligned} \quad (4.7)$$

$$u^C \nabla_C \Omega_{AB} = -\frac{2}{n-1} \Theta \Omega_{AB} - 2 \Sigma^C_{[B} \Omega_{A]C} \quad (4.8)$$

where $\Sigma^2 = \Sigma_{AB} \Sigma^{AB}$, $\Omega^2 = \Omega_{AB} \Omega^{AB}$, W_{CBAD} is the Weyl tensor and the quantity $\tilde{R}_{AB} = h_{AC} h_{BD} R^{CD} - \frac{1}{n-1} h_{AB} h_{CD} R^{CD}$. One can analyse the above equations for special cases, as we shall see below.

A. Randall–Sundrum warp factor with and without branes

It is known that in Einstein spaces, we have $R_{AB} \sim g_{AB}$ and all the components of the Weyl tensor as well as \tilde{R}_{AB} vanish. Therefore the equation for the expansion simplifies considerably if we set $\Sigma_{AB} = \Omega_{AB} = 0 \forall A, B$. Following this prescription for the RS scenario [4, 5] in the absence of any brane, Eq. 4.6 gives us

$$\frac{d\Theta}{d\lambda} + \frac{\Theta^2}{4} = \frac{\Lambda}{6M^3} \quad (4.9)$$

where, Λ is the bulk cosmological constant and M is the five dimensional Planck mass. Let us further assume $\Theta = 4 \frac{\dot{F}}{F}$ (notion of focusing is related to $F = 0$, $\dot{F} < 0$ at finite λ), which leads to

$$\ddot{F} + k^2 F = 0, \quad \text{with} \quad k = \sqrt{\frac{-\Lambda}{24M^3}}, \quad (4.10)$$

As discussed in [5], Λ has to be negative. Eq.4.10 has simple oscillatory solutions such as $c_1 \sin(k\lambda + c_2)$, which imply $\Theta = 4k \cot(k\lambda + c_2)$. Therefore, the nature of focusing or defocusing of geodesics in the bulk depends on the initial condition or the value of c_2 . However, this is the behavior of geodesic congruences in the bulk with no branes. If we introduce two 3-branes, the hidden brane (with positive tension $24M^3 k$) at $\sigma = 0$ and the visible brane (with equal negative tension) at $\sigma = \pi$, Eq.4.10 becomes

$$\ddot{F} + [k^2 + 2k\{\delta(\sigma) - \delta(\sigma - \pi)\}] F = 0. \quad (4.11)$$

Using the following property of Dirac delta function

$$\delta(\sigma(\lambda)) = \sum_i \frac{\delta(\lambda - \lambda_i)}{|\dot{\sigma}(\lambda_i)|}, \quad (4.12)$$

and the first integral of the σ geodesic equation

$$\dot{\sigma} = \sqrt{C^2 e^{-2f} - 1} \quad \text{with} \quad f(\sigma) = -k|\sigma|, \quad (4.13)$$

we arrive at

$$\ddot{F} + [k^2 + k_1\delta(\lambda - \lambda_0) - k_2\delta(\lambda - \lambda_\pi)] F = 0, \quad (4.14)$$

where, $k_1 = \frac{2k}{\sqrt{C^2-1}}$, $k_2 = \frac{2k}{\sqrt{C^2e^{2k\pi}-1}}$, $\lambda_0 = \frac{\sec^{-1}C}{k}$ and $\lambda_\pi = \frac{\tan^{-1}\sqrt{C^2e^{2k\pi}-1}}{k}$. The solution of the above equation is given by [24]

$$F(\lambda) = c_1 \sin(k\lambda + c_2) + c_3 e^{-\alpha|\lambda-\lambda_0|} + c_4 e^{-\alpha|\lambda-\lambda_\pi|} \quad (4.15)$$

where c_1, c_2, c_3, c_4 are arbitrary constants. We then integrate the second order equation for F , around the neighborhood of λ_0 and λ_π to obtain two algebraic equations for c_1 and c_2 . The determinant condition for nontrivial solutions of c_1, c_2 yields the following transcendental equation,

$$(2\alpha - k_1)(2\alpha + k_2) + k_1 k_2 e^{-2\alpha(\lambda_\pi - \lambda_0)} = 0. \quad (4.16)$$

from which α can be obtained numerically. In our case, $\alpha \sim k_1/2$ is a good approximation (we have checked this with numerical solutions as well). Fig.1 shows (shaded regions) the domain of the parameters c_3/c_1 and c_4/c_1 , while c_2 is taken to be zero, in cases where $F = 0$ at some finite value of λ in between the two branes. Points on the boundary correspond to location of the branes. In the lightly shaded region, $\dot{F} > 0$, which implies complete defocusing of geodesics, whereas in the darker region, $\dot{F} < 0$, i.e. geodesic focusing occurs. Note that different values for c_2 will result in different parameter space diagrams for c_3/c_1 and c_4/c_1 . Eq.4.15 leads to the modified expansion scalar, due to the presence of the branes,

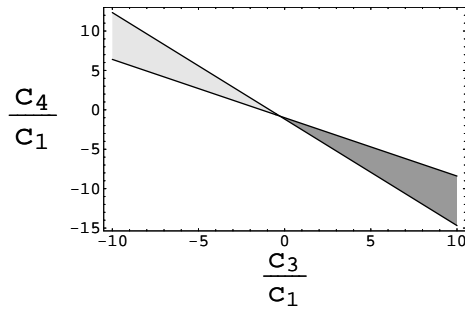


FIG. 1: Values of c_3/c_1 and c_4/c_1 lying in the shaded region corresponds to focusing (deeply shaded) and defocusing (lightly shaded) of geodesics in between the brane locations

as given by

$$\Theta(\lambda) = 4 \frac{c_1 k \cos(k\lambda + c_2) - c_3 \alpha \operatorname{sgn}(\lambda - \lambda_0) e^{-\alpha|\lambda-\lambda_0|} - c_4 \alpha \operatorname{sgn}(\lambda - \lambda_\pi) e^{-\alpha|\lambda-\lambda_\pi|}}{c_1 \sin(k\lambda + c_2) + c_3 e^{-\alpha|\lambda-\lambda_0|} + c_4 e^{-\alpha|\lambda-\lambda_\pi|}}. \quad (4.17)$$

Due to the new integration constants, the behavior of geodesic congruences have become much richer. In Fig.2(a) and Fig.2(b) two such examples are shown using typical values of the parameters and constants. It is clear from these figures, how the existence of branes

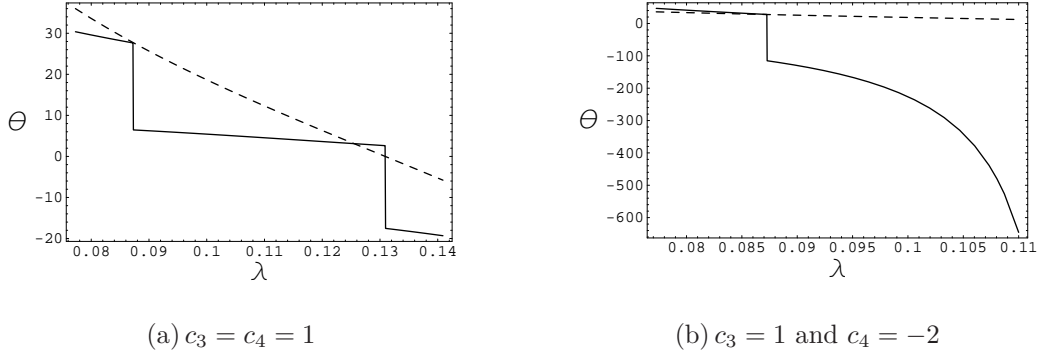


FIG. 2: Evolution of expansion scalar in presence (continuous line) and in absence (dotted line) of two 3-branes with $k = 12$, $C = 2$, $c_1 = 1$, $c_2 = 0$ and $\alpha = 6.9282$ (from Eq.4.16).

modifies the expansion profiles.

After this brief discussion on geodesic flows in the RSI scenario, we will now address the problem of solving the Raychaudhuri equations in a generalised braneworld scenario, with a thick cosmological brane and a time dependent extra dimension. Our main aim is to point out the specific roles of the different metric functions which appear in the line element on the evolution of geodesic congruences.

B. ESR from definitions

As mentioned before, one can derive analytic expressions for the ESR variables directly from the definitions, Eq.4.2 - Eq.4.4, using the geodesic vector field components obtained in Section III. We now illustrate the nature of the ESR for some specific cases, where we take one or two of the metric functions as constants.

1. Case 1

With $a(\eta) = b(\eta) = \text{constant}$, i.e. the metric given by

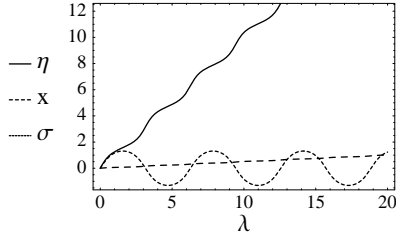
$$ds^2 = e^{2f(\sigma)} [-d\eta^2 + d\mathbf{X}^2] + d\sigma^2, \quad (4.18)$$

the corresponding velocity vector components for timelike geodesics are given by

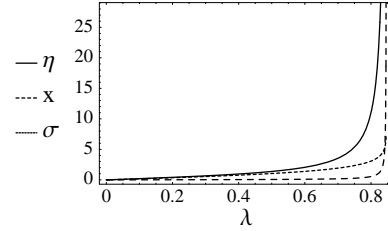
$$u^\alpha = C_\alpha e^{-2f} \quad \text{where} \quad \alpha = 0, 1, 2, 3 \quad (4.19)$$

$$u^4 = \sqrt{C^2 e^{-2f} - 1} \quad \text{where} \quad C^2 = C_0^2 - \sum_{i=1}^3 C_i^2, \quad (4.20)$$

where the C_α 's are integration constants, which are constrained by the fact that u^4 has to be real valued. Fig.3 shows the nature of timelike geodesics in the presence of growing and decaying warp factors. Clearly, the geodesics are bounded along the σ direction in the case of a growing warp factor and the boundaries are given by $|\sigma| = \text{sech}^{-1}(1/C)$. However this is not the situation with a decaying warp factor, though λ itself is bounded. For a detailed study of geodesics in generalised braneworld scenarios, see [6]. The scalar function,



(a) With growing warp factor.



(b) With decaying warp factor.

FIG. 3: Evolution of the components of timelike geodesics for growing and decaying warp factors with both $a(\eta) = b(\eta) = \text{constant}$.

Φ , defined in the previous section, for the case with a decaying warp factor is given by

$$\Phi(x^A) = \sum_{\alpha=0}^3 C_\alpha x^\alpha - i\sqrt{C^2 - 1} \text{EllipticE} \left[i\sigma, \frac{C^2}{C^2 - 1} \right] + C_4, \quad (4.21)$$

where C_4 is an integration constant. Similarly, one can find this scalar for other cases, too when the rotation is zero.

According to the definitions Eq.4.2 - Eq.4.4, the expansion scalar and the other ESR variables for a congruence of timelike geodesics, found as functions of σ , are given as follows,

$$\Theta = \frac{3C^2 e^{-2f} - 4}{\sqrt{C^2 e^{-2f} - 1}} f', \quad (4.22)$$

$$\begin{aligned}
\Sigma_{00} &= \frac{C_0^2(4 - 3C^2e^{-2f}) - C^2}{4\sqrt{C^2e^{-2f} - 1}}f', & \Sigma_{ii} &= \frac{C_i^2(4 - 3C^2e^{-2f}) + C^2}{4\sqrt{C^2e^{-2f} - 1}}f', \\
\Sigma_{44} &= -\frac{3C^4f'e^{-4f}}{4\sqrt{C^2e^{-2f} - 1}}, & \Sigma_{\alpha i} &= -\frac{C_\alpha C_i(3C^2e^{-2f} - 4)}{4\sqrt{C^2e^{-2f} - 1}}f' \text{ for } \alpha \neq i, \\
\Sigma_{\alpha 4} &= -\frac{C_\alpha}{4}3C^2f'e^{-2f}, & \Sigma^2 &= \frac{3C^4e^{-4f}f'^2}{4(C^2e^{-2f} - 1)} \quad \text{and} \quad \Omega_{AB} = 0 \forall A, B.
\end{aligned} \tag{4.23}$$

For growing and decaying warp factor respectively, the expansion scalar becomes

$$\Theta_+ = \frac{3C^2 \operatorname{sech}^2 \sigma - 4}{\sqrt{C^2 \operatorname{sech}^2 \sigma - 1}} \tanh \sigma \quad \text{and} \quad \Theta_- = -\frac{3C^2 \cosh^2 \sigma - 4}{\sqrt{C^2 \cosh^2 \sigma - 1}} \tanh \sigma. \tag{4.24}$$

It can be easily seen that, in the region $\dot{\sigma} > 0$, irrespective of the value of C , $\Theta_\pm \rightarrow -\infty$ as σ increases. Therefore a geodesic congruence singularity arises in both the cases. With Θ_+ , if $C > \sqrt{4/3}$, initially the expansion remains positive but eventually geodesics meet exactly at the boundary of the accessible domain along the extra dimension because the velocity component along σ , u^4 , which appears in the denominator in the expression for Θ , vanishes at that point (and also changes sign). With Θ_- , the geodesic congruence singularity appears as $\sigma \rightarrow \infty$. For $\dot{\sigma} < 0$ an exactly same behavior is obtained. The following figures illustrate the nature of the expansion and shear in presence of growing and decaying warp factors. The corresponding geodesics in Fig.3 tell us that Θ_+ experiences a finite time singularity (i.e. finite λ as well as finite σ) but Θ_- becomes singular at finite λ but $\eta, \sigma \rightarrow \infty$. The

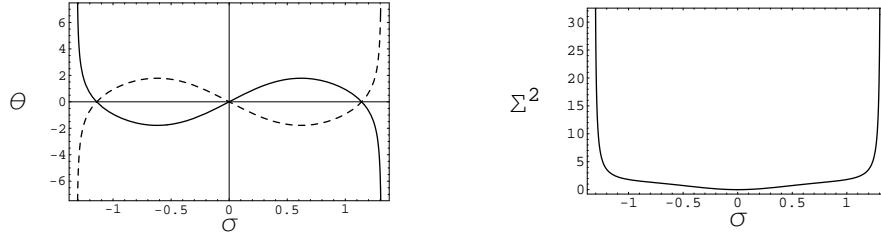


FIG. 4: Nature of expansion ($\dot{\sigma} > 0$: continuous, $\dot{\sigma} < 0$: dashed) and shear in presence of growing warp factor with $C = 1.31$.

continuous and dashed curves in the plots of Θ vs. σ stand for geodesics with positive u^4 (moving towards positive σ direction) and negative u^4 (moving towards negative σ direction) respectively. In both cases congruence singularities are inevitable. The evolutions of Σ^2 in these scenarios, plotted in Fig.4 and Fig.5, follow from its expression as given in Eq.4.23.

To understand how geodesic focusing in all the abovementioned scenarios are physically realised, let us consider the evolution of the projections of the cross-sectional area orthogonal

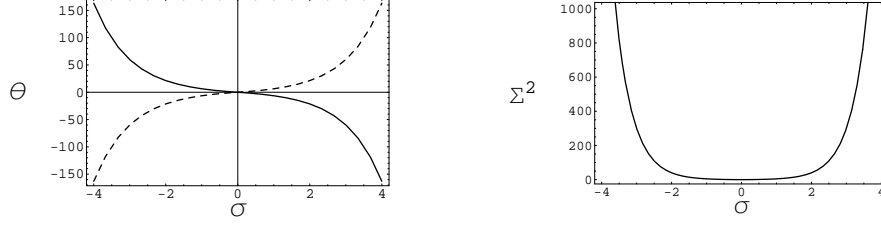


FIG. 5: Nature of expansion ($\dot{\sigma} > 0$: continuous, $\dot{\sigma} < 0$: dashed) and shear in presence of decaying warp factor with $C = 1.31$.

to the flow lines, of a congruence of four geodesics, on different four dimensional surfaces. This is done by numerically solving the following equation for the deviation vector along with Eq.4.5 and Eq.3.3,

$$\xi^A_{;B} u^B = B^A_B \xi^B. \quad (4.25)$$

Here, ξ^A represents the separation between two neighboring geodesics. To see the evolution from a local observer's viewpoint, we have to express the tensorial quantities in the frame basis. The metric tensor in coordinate basis and frame basis are related as

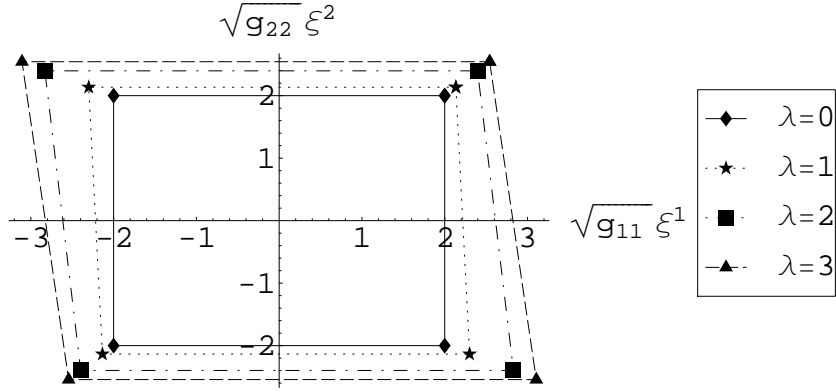
$$g^{AB} = e^A_a e^B_b \eta^{ab}, \quad (4.26)$$

where the vierbein field, e^A_a , has two indices, “A” labels the general spacetime coordinate (w.r.t. the coordinate basis) and “a” labels the local Lorentz spacetime or local laboratory coordinates (w.r.t. the frame basis). The tensorial components in these two bases are related as

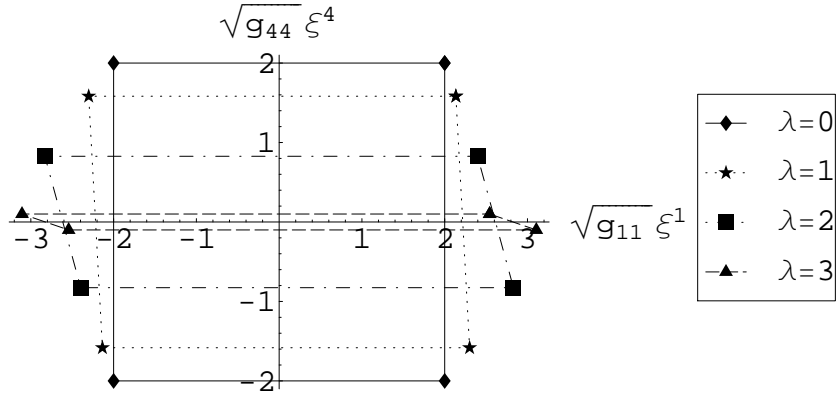
$$\xi^A = e^A_a \xi^a. \quad (4.27)$$

In the frame basis, we set the initial conditions such that, at $\lambda = 0$, projected area has the shape of a square in the $\sqrt{g_{11}}\xi^1$ - $\sqrt{g_{22}}\xi^2$ plane or in the $\sqrt{g_{11}}\xi^1$ - $\sqrt{g_{44}}\xi^4$ plane. The following figures show the evolution of the area elements as λ increases. We have chosen initial conditions such that all the rotation parameters vanish.

Fig.6 shows how a projected 2D square element evolves, in a static bulk, in presence of a growing warp factor i.e. the scenario addressed in Fig.4. In Fig.6(a), the initial square area (at $\lambda = 0$) in the $\sqrt{g_{11}}\xi^1$ - $\sqrt{g_{22}}\xi^2$ plane expands and distorts slightly and converges on a parallelogram at $\lambda \sim 3.14$. In Fig.6(b), however the area in the $\sqrt{g_{11}}\xi^1$ - $\sqrt{g_{44}}\xi^4$ plane shrinks, distorts and converges on the $\sqrt{g_{11}}\xi^1$ axis at $\lambda \sim 3.14$, clearly suggesting focusing along the



(a) Evolution of the projected square element on $\sqrt{g_{11}}\xi^1$ - $\sqrt{g_{22}}\xi^2$ plane

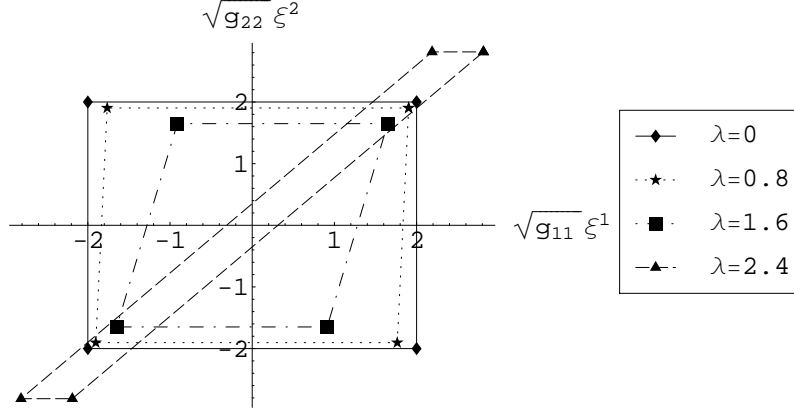


(b) Evolution of the projected square element on $\sqrt{g_{11}}\xi^1$ - $\sqrt{g_{44}}\xi^4$ plane

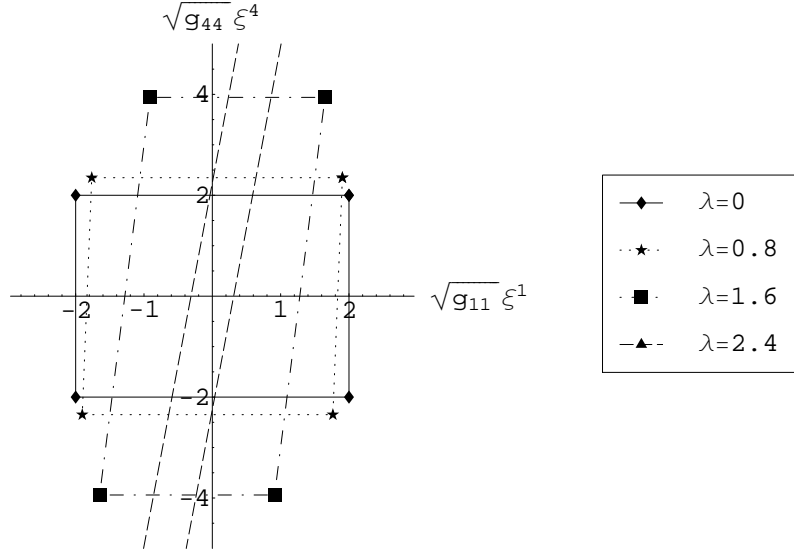
FIG. 6: Evolution of different 2D surface elements in Case 1 in presence of a growing warp factor

extra dimension. The effect of shear is evident from the evolution of the shape of the area. Note that, Fig.3 shows that the geodesics turn around from the boundary ($\sigma(\lambda)$, reaches maximum at $\lambda \sim 3.14$) and oscillate along the extra dimension (duration between $\lambda = 0$ and $\lambda = 3.14$ corresponds to one-fourth of a period of oscillation of $\sigma(\lambda)$). This implies that the evolution in Fig.6 will evolve in the opposite direction and square area element will again be formed at $\lambda \sim 6.28$. This evolution repeats itself as λ goes on.

On the other hand, Fig.7 corresponds to the scenario addressed in Fig.5, where the warping factor is decaying. In Fig.7(a), shrinking of the area element is prominent whereas in Fig.7(b) it is not very evident. But in both the figures, the square area become more and more parallelogram shaped and eventually converge on a line $\sqrt{g_{11}}\xi^1 \propto \sqrt{g_{22}}\xi^2$ or $\sqrt{g_{11}}\xi^1 \propto \sqrt{g_{44}}\xi^4$ as $\lambda \rightarrow \infty$.



(a) Evolution of the projected square element on $\sqrt{g_{11}}\xi^1$ - $\sqrt{g_{22}}\xi^2$ plane



(b) Evolution of the projected square element on $\sqrt{g_{11}}\xi^1$ - $\sqrt{g_{44}}\xi^4$ plane

FIG. 7: Evolution of different 2D surface elements in Case 1 in presence of a decaying warp factor.

The nature of evolution of the square elements is indeed a distinguishing feature between bulk universes with growing and decaying warp factors. It is worth mentioning here that, to a brane based observer, only the evolution depicted in Fig.6(a) or Fig.7(a) will be visible whereas congruence singularities realised in Fig.6(b) or Fig.7(b) will remain unnoticed.

2. Case 2

Next, we consider the case where $f(\sigma) = \text{constant}$, i.e. the metric looks like

$$ds^2 = a^2(\eta) [-d\eta^2 + d\mathbf{X}^2] + b^2(\eta) d\sigma^2. \quad (4.28)$$

Integral curves are given by the following velocity vector field

$$\begin{aligned} u^i &= \frac{C_i}{a^2}, & u^4 &= \frac{C_4}{b^2}, \\ u^0 &= \sqrt{\frac{1}{a^2} + \sum_{i=1}^3 \frac{C_i^2}{a^4} + \frac{C_4^2}{a^2 b^2}} \end{aligned} \quad (4.29)$$

Accordingly the expansion scalar is derived as

$$\Theta = -\frac{1}{u_0} \left[3\frac{\dot{a}}{a} + 2\sum_i \frac{C_i^2 \dot{a}}{a^3} + \frac{3C_4^2 \dot{a}}{ab^2} + \frac{\dot{b}}{b} + \sum_i \frac{C_i^2 \dot{b}}{a^2 b} \right]. \quad (4.30)$$

Similarly one can calculate the components of shear (which are not shown here). Rotation parameters are found to be zero as is evident from the velocity field. Fig.8 and Fig.9 show the evolution of expansion scalar and Σ^2 as functions of η for two different $a(\eta), b(\eta)$ combinations i.e. Set(A) and Set(B) respectively. In Fig.8 (Set(A)), geodesics become parallel as $\eta \rightarrow \infty$.

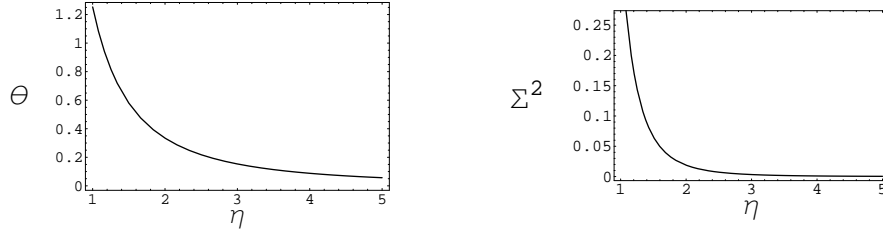


FIG. 8: Nature of expansion and shear in Case 2 for Set(A), with $C_i = C_4 = 0.1$

This is because with Set(A), expansion of the universe itself slows down with increasing η (it is worth mentioning here that as the cosmological evolution is assumed to begin at a finite η , the past singularity will not appear here as that event corresponds to $\eta = 0$ and falls outside the regime of the models considered in this article) whereas, for Set(B), Fig.9 shows that the geodesics spread apart at an ever increasing rate as η increases – this is due to very rapid expansion of the universe. In both these cases geodesic focusing is not achieved. On the other hand, in the previous section we have seen that geodesic singularities are unavoidable when only the warping factor is assumed as non-constant in the line element. Therefore, it

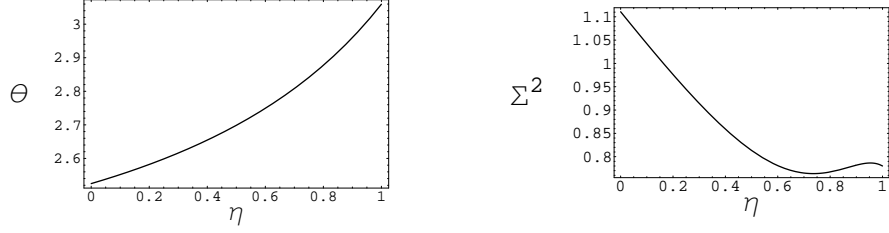


FIG. 9: Nature of expansion and shear in Case 2 for Set(B), with $C_i = C_4 = 0.1$

should be interesting to see how the two apparently opposite behaviors compete with each other when we consider the full braneworld geometry with all three metric functions present.

To figure out the individual effect of the dynamic nature of $b(\eta)$, we take $a(\eta)$ to be a constant in Eq.4.30 to get

$$\Theta = \frac{(1 + \sum_i C_i^2) \dot{b}}{\sqrt{(1 + \sum_i C_i^2) b^2 + C_4^2}}. \quad (4.31)$$

In our models \dot{b} is negative and as η increases it tends to zero. For $b(\eta)$ of Set(A), Θ tends to zero i.e. geodesics become parallel and for Set(B) it converges on a finite value which means geodesics keep on moving away from each other at an approximately steady rate. So, in both cases geodesic focusing never happens. It is interesting to note that even if $b(\eta) \rightarrow 0$ i.e. size of the extra dimension becomes singular the expansion scalar remains finite as long as \dot{b} is finite. Therefore we expect $b(\eta)$ to play a role only in introducing a scaling effect. This will be apparent when we consider the scenario with all three metric functions involved.

Analytic expressions for the first integrals of the geodesic equations for the case with both $f(\sigma)$ and $a(\eta)$ present can also be found easily. But, in this case, the ESR variables as obtained from the definitions given in Eq.4.2-4.4 are functions of both σ and η . Further they cannot be reduced to explicit functions of λ (or σ , η) alone. This happens because we do not know how $\sigma(\lambda)$ and $\eta(\lambda)$ are related to each other (analytically). Thus, the above two subcases (of a generalised braneworld geometry) are the only ones where one can find useful analytic expressions for the ESR variables directly from the velocity vector field.

C. Numerical solutions

Here we numerically solve Eq.4.5 simultaneously with Eq.3.3 for different combinations of the metric functions in order to understand the interplay amongst all the terms appearing in the Raychaudhuri equations. Looking at Eq.4.6, one sees that, the “ Ω^2 ” term has an

opposite effect as compared to the shear term. Thus, it may play a role in avoiding/delaying congruence singularities found in the earlier section. On the other hand, the curvature term “ $R_{AB}u^A u^B$ ”, in Eq.4.6, also has a significant effect on ESR profiles through its large positive or negative value at some point.

We have analysed each case for essentially two types of initial conditions – one with zero rotation and one with very high initial rotation keeping initial Θ and Σ_{AB} as zero. Non-zero initial values for Ω_{AB} are chosen such that $\Omega_{AB}u^B = 0 = u^A\Omega_{AB}$ at $\lambda = 0$. Initial velocities for cases involving Set(A) scale factors are taken as $\{0.728, 0.1, 0.1, 0.1, 0.5\}$, whereas for Set(B), it is assumed as $\{1.1314, 0.1, 0.1, 0.1, 0.5\}$ to satisfy the timelike constraint for the geodesics. Let us analyse the results graphically. In the following figures (Fig.10-Fig.13), the subfigures (a) and (b) contain *dual-axis* plots where the continuous curves (axes) represent evolution with zero initial rotation and the dashed curves (axes) represent evolution with high initial rotation.

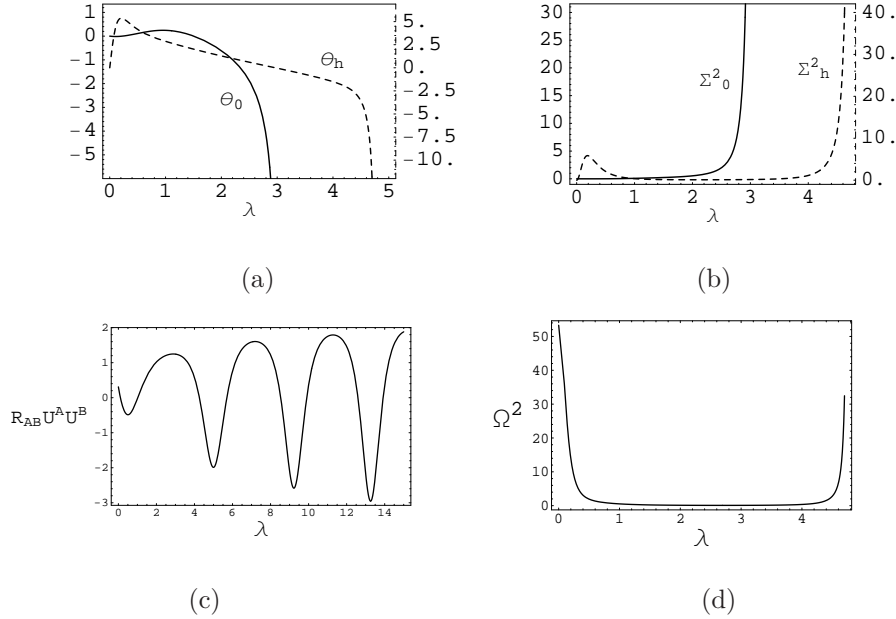


FIG. 10: Nature of expansion, shear and rotation for $f(\sigma) = \log(\cosh \sigma)$, $a(\eta) = 2\eta$ and $b(\eta) = 1 + 1/\eta$ with two different set of initial conditions. In (a) and (b), subscripts 0 (h) correspond to zero (high) initial rotation.

Fig.10: In the presence of a growing warp factor, a radiative brane and an asymptotically static extra dimension, the geodesic congruence, without any initial rotation, expands slowly at first but later becomes focused at a finite λ . The shear (Σ^2) grows indefinitely. When

high initial rotation is introduced, expansion inflates for a very short while but eventually the geodesics get focused again at another finite but larger value of λ . Though rotation increases at late times, it is always dominated by shear, which grows even faster. Initial rotation only succeeds in delaying the focusing. The curvature term is not an important factor here.

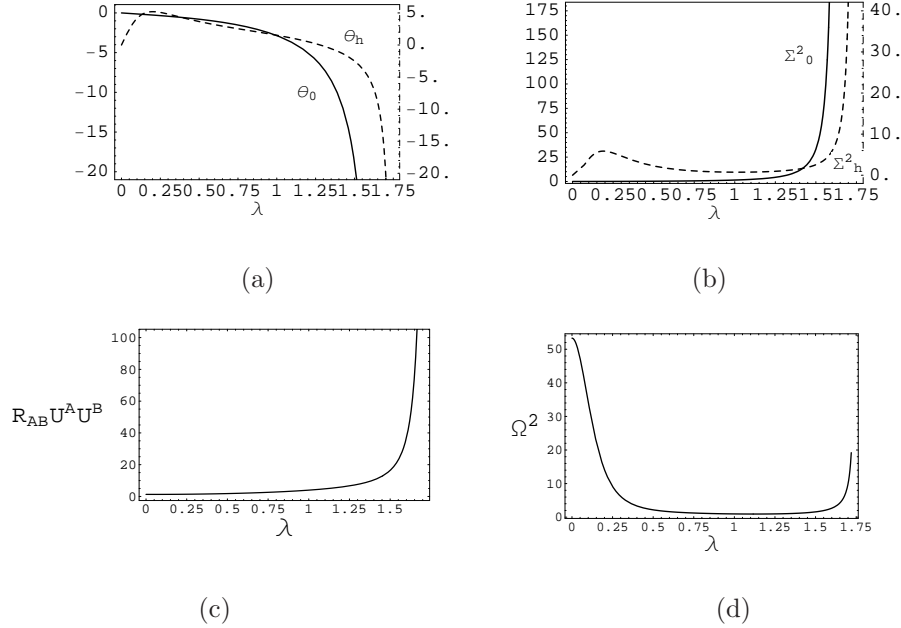


FIG. 11: Nature of expansion, shear and rotation for $f(\sigma) = -\log(\cosh \sigma)$, $a(\eta) = 2\eta$ and $b(\eta) = 1 + 1/\eta$ with two different set of initial conditions. In (a) and (b), subscripts 0 (h) correspond to zero (high) initial rotation.

Fig.11: In the presence of a decaying warp factor, a radiative brane and an asymptotically static extra dimension the geodesics, without any initial rotation, monotonically come closer and tend to focus as $\sigma \rightarrow \infty$. The shear grows indefinitely. When high initial rotation is introduced, the congruence expands initially but eventually geodesics tend to focus again asymptotically. The curvature term becomes large positive valued and thus always helps the occurrence of congruence singularity.

Fig.12 represents almost the same behavior as we have seen in Fig.10. But here the large initial rotation decays down very quickly. The physical reason behind this is the very fast expansion of spacetime that smears out all the initial rotation components.

Fig.13: In the presence of a decaying warp factor, a de Sitter brane with an asymptotically static extra dimension, we have an example where geodesics are defocused irrespective of

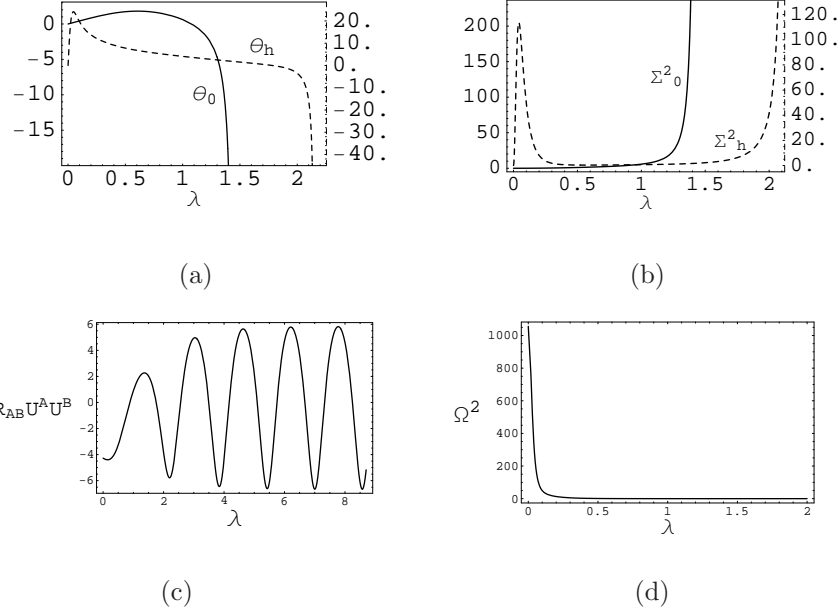


FIG. 12: Nature of expansion, shear and rotation for $f(\sigma) = \log(\cosh \sigma)$, $a(\eta) = 1/(1 - \eta)$ and $b(\eta) = 1 - \eta/2$ with two different set of initial conditions. In (a) and (b), subscripts 0 (*h*) correspond to zero (high) initial rotation.

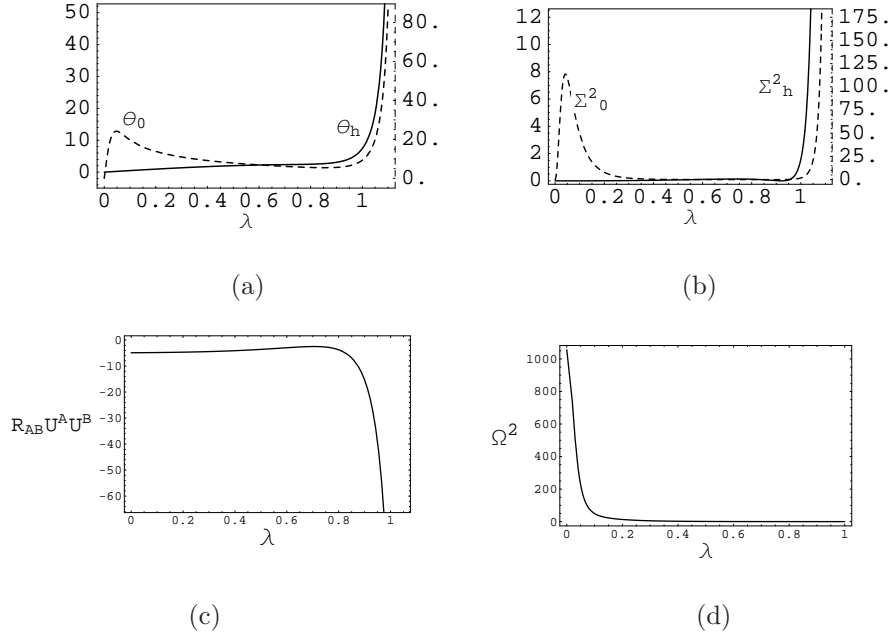


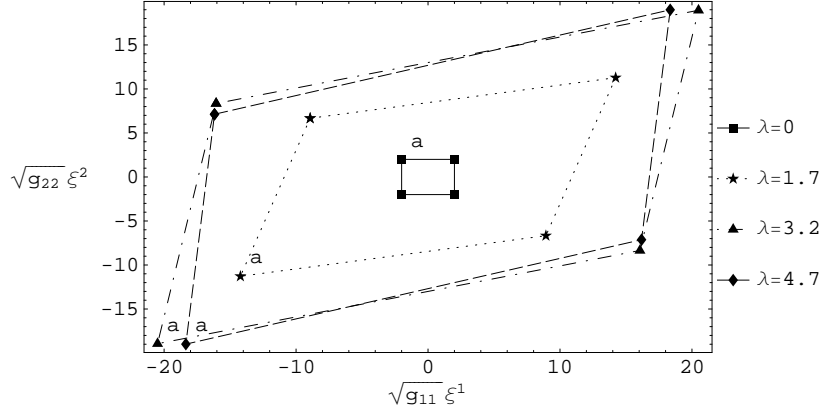
FIG. 13: Nature of expansion, shear and rotation for $f(\sigma) = -\log(\cosh \sigma)$, $a(\eta) = 1/(1 - \eta)$ and $b(\eta) = 1 - \eta/2$ with two different set of initial conditions. In (a) and (b), subscripts 0 (*h*) correspond to zero (high) initial rotation.

initial rotation. Even though it seems that at late times shear totally dominates rotation,

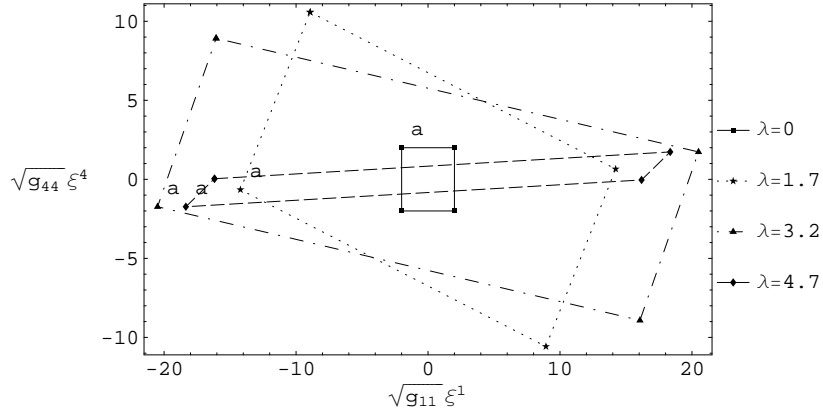
it is the curvature term in the Raychaudhuri equation that becomes dominant and causes the defocusing. Remember that, with $a(\eta) = b(\eta) = \text{constant}$, congruence singularity was inevitable (Fig.5). On the other hand, Fig.13(c) shows that initially the curvature term is very small which implies that a high enough initial negative expansion should lead to a congruence singularity at a finite λ (before the curvature term becomes dominant). This behavior has been checked with an initial expansion, $\Theta = -30$ (figure not shown).

From the results in Fig.10-Fig.13, one can draw some general conclusions about the nature of the ESR variables. Congruence singularity is inevitable in the cases addressed in Fig.10 and Fig.12, i.e. for growing warp factor with Set(A) and Set(B) scale factors. Even a large amount of initial rotation, too, fails to resolve the congruence singularity. This is because, in presence of growing warp factor, the geodesics have a turning point in the extra dimension. This fact forces the congruence singularity to occur at that point. Using different kinematic properties, such as high initial expansion, is not going to resolve this singularity. Fig.11 represents a case where the geodesics are not bounded. Even a high initial expansion cannot make the congruence to diverge. On the other hand, the geodesics are divergent when $f(\sigma) = -\log(\cosh \sigma)$, $a(\eta) = 1/(1-\eta)$ and $b(\eta) = 1-\eta/2$ (Fig.13), which corresponds to a negatively warped and exponentially expanding brane. It is interesting to note that defocusing happens irrespective of the value of “ Ω^2 ”. This is because the term, in the right hand side of Eq.4.6, “ $R_{AB}u^A u^B$ ” becomes dominant and large negative (which is not the case with other combinations of the metric functions) as λ increases (Fig.13(c)). Therefore one can say that this defocusing is purely an effect of the spacetime geometry and congruence singularity can be achieved with initially high negative expansion. Also note that, the dashed curves in Figs 10(a), 11(a), 12(a) and 13(a) show that even if we begin with a large initial rotation, at the end, shear dominates. Initially, expansion remains positive which is entirely because of high initial rotation.

Now let us look at the evolution of congruence of geodesics from the local observer’s point of view and how the ESR profiles, plotted in Figs10-13, are realised. As we have done earlier, here also we have plotted the evolution of square elements, orthogonal to the congruence of the timelike geodesics, projected on $\sqrt{g_{11}}\xi^1$ - $\sqrt{g_{22}}\xi^2$ and $\sqrt{g_{11}}\xi^1$ - $\sqrt{g_{44}}\xi^4$ planes. These plots actually give us a different perspective of the evolution as it involves different shear and rotation tensor components. Here we have labeled one point of the square element (one in the second quadrant initially) as “a”, so that following its location on future quadrilaterals



(a) Evolution of the projected square element on $\sqrt{g_{11}}\xi^1 - \sqrt{g_{22}}\xi^2$ plane

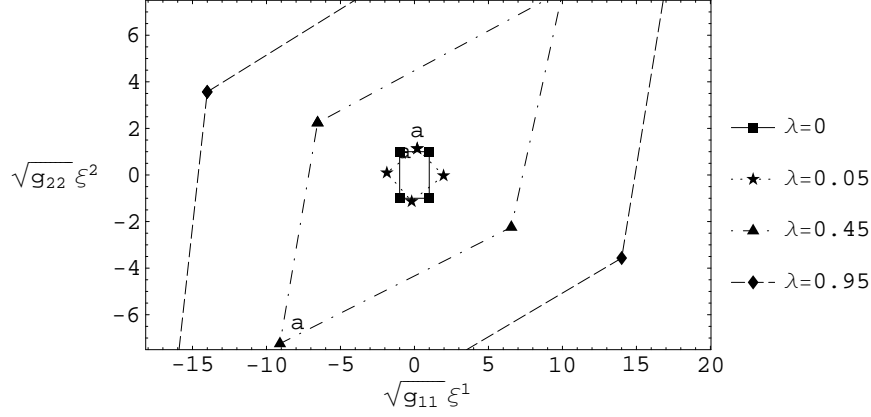


(b) Evolution of the projected square element on $\sqrt{g_{11}}\xi^1 - \sqrt{g_{44}}\xi^4$ plane

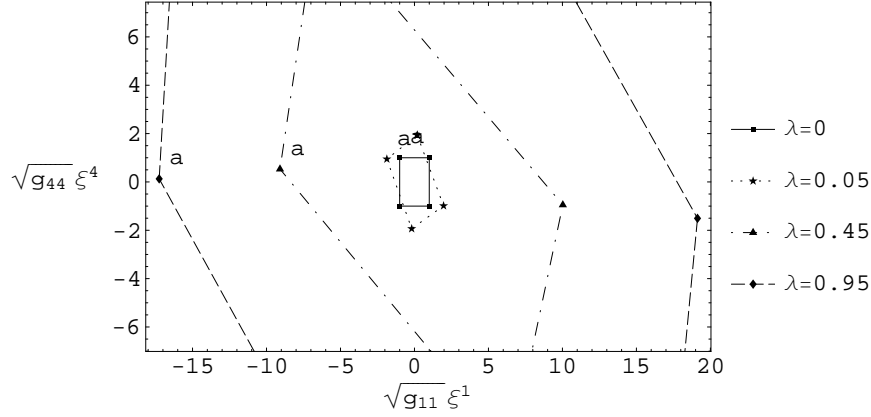
FIG. 14: Evolution of different 2D surface elements for $f(\sigma) = \log(\cosh \sigma)$, $a(\eta) = 2\eta$ and $b(\eta) = 1 + 1/\eta$ with $\Theta = \Sigma^2 = 0$ and $\Omega^2 \sim 54$ at $\lambda = 0$

(with increasing λ) one can find the effect of rotation.

Fig.14 corresponds to the evolution of the dashed curve in Fig.10(a). Fig.14(a) suggests the following. Initially, the area element expands very quickly due to large amount of rotation which is also clearly visible. At the end rotation starts to increase again after slowing down a little at the middle and the area starts to shrink too. Amount of shear also increases initially though towards the end it starts to decrease. In Fig.14(b) shrinking of the area element after an initial expansion, increase in the amount of shear after a decrease at the middle and a quick decrease in rotation are more clearly visible. As we have pointed out earlier, in presence of a growing warp factor, the evolution will repeat itself.



(a) Evolution of the projected square element on $\sqrt{g_{11}}\xi^1 - \sqrt{g_{22}}\xi^2$ plane



(b) Evolution of the projected square element on $\sqrt{g_{11}}\xi^1 - \sqrt{g_{44}}\xi^4$ plane

FIG. 15: Evolution of different 2D surface elements for $f(\sigma) = -\log(\cosh \sigma)$, $a(\eta) = 1/(1 - \eta)$ and $b(\eta) = 1 - \eta/2$ with $\Theta = \Sigma^2 = 0$ and $\Omega^2 \sim 1080$ at $\lambda = 0$

Fig.15 represents the evolution of the dashed curve in Fig.13(a). In both the plots, the area of the quadrilateral keeps on increasing with λ . Effect of high initial rotation is prominent, so is its rapid decrease. Effect of shear in Fig.15(b) matches with the profile of Fig.13(b), though this is not exactly the case with Fig.15(a). As we have mentioned earlier, these qualitatively different ESR evolutions may easily be in one to one correspondence with different models. This, in turn, points toward possible verification of those models through observations.

Warp factor $e^{2f(\sigma)}$	Constant $a(\eta)$, $b(\eta)$ (Analytical results)	$a(\eta) = 2\eta$, $b(\eta) = 1 + 1/\eta$ (Radiative)	$a(\eta) = 1/(1 - \eta)$, $b(\eta) = 1 - \eta/2$ (de Sitter)
Growing	Congruence singularity at finite σ (Fig.4)	Congruence singularity at finite σ (Fig.10)	Congruence singularity at finite σ (Fig.12)
Decaying	Congruence singularity at $\sigma \rightarrow \infty$ (Fig.5)	Congruence singularity at $\sigma \rightarrow \infty$ (Fig.11)	Defocusing at $\sigma \rightarrow \infty$ (Fig.13) or congruence singularity at finite σ for large, -ve initial Θ
Constant	–	No congruence singularity (Fig.8)	No congruence singularity (Fig.9)

TABLE I: Summary of behaviour of geodesic congruences for different metric coefficients

V. DISCUSSION

In this article we have analysed, in detail, the kinematics of timelike geodesics in a generalised braneworld scenario where we have a background five dimensional bulk with a warped cosmological brane and an extra dimension whose size is time dependent. We now briefly summarize the work done, the results obtained and possibility of future investigations.

- We have considered different functional forms for the metric functions, namely $f(\sigma)$: the warp factor, $a(\eta)$: the cosmological scale factor and $b(\eta)$: the scale factor attached with the extra dimension. The four types of combinations give us four different viable braneworld scenarios with a cosmological (thick) brane. Geodesic flows in these backgrounds governed by the Raychaudhuri equations are then solved. Analytic solutions are possible only for few simpler cases where one takes one or two of the metric functions as constants. The simplification in fact helps us to explicitly distinguish the effect of individual metric functions when we compare the results with the numerical solutions, where, all the metric functions are considered.
- The interplay among different metric functions e.g. effect of warping and cosmological expansion of the brane is clearly visible in the results. In general, growing warp factor leads to a finite η (and σ) congruence singularity whereas in the presence of a decaying warp factor, geodesics are focused at η (and σ) $\rightarrow \infty$. In a radiative universe (where

$a(\eta) \sim \eta$), things do not change qualitatively. But in a de Sitter universe (where $a(\eta) \sim 1/(1 - \eta)$), negative warp factor fails to focus the geodesics, though this is not the case when the brane is positively warped. Thus, one may say that the above is a purely geometric effect. Therefore, when the curvature effect is relatively small, congruence singularity is achievable for high enough negative initial expansion.

The effect of initial rotation, on the ESR profiles, especially the expansion scalar, is found to be quantitative. In cases with focusing without any initial rotation as well as with large initial rotation, similar results are obtained, though with large initial rotation, geodesics tend to spread for a while (focusing at larger λ value). The above conclusions are summarised in Table I.

- We have plotted the evolution of a square element that represents the surface orthogonal to a geodesic congruence, from a local observer's point of view. This helps one to visualise exactly how the expansion, shear and rotation behave along the congruences.
- The effect of a dynamic extra dimension i.e. the role of $b(\eta)$ seems to be only quantitative. This is because in these models as λ evolves $b(\eta)$ tends to a static value with a deceleration. For a different dynamic nature of the extra dimension one is bound to get different results.
- A small sub-section is devoted to the discussion on a special case –the RS two brane scenario (bulk Einstein space). In this case, the equations become analytically solvable when shear and rotation components are consistently assumed to vanish. Introduction of branes considerably changes the expansion profile of geodesic congruences. Depending on the values of the new parameters introduced (i.e. the initial conditions) both focusing and defocusing can arise in the region between the branes. We have also pointed out, through a parameter space diagram, which initial conditions in the parameter space give rise to such behavior.

In our work here, we have considered a congruence of timelike geodesics. It might be more interesting to see what happens for null geodesic congruences. In such a scenario, one can directly analyse the results in the context of gravitational lensing of light rays and distinguish the individual effects of the warp factor as well as the other metric functions.

Acknowledgments

SG thanks Council for Scientific & Industrial Research (CSIR), India for providing financial support and Centre for Theoretical Studies, IIT Kharagpur, India for allowing him to use its research facilities.

-
- [1] Th. Kaluza, Sitzunober. Preuss. Akad. Wiss. Berlin, 966 (1921); O. Klein, Z. Phys. **37** (1926) 895
 - [2] M. S. Green, J. H. Schwarz and E. Witten, *Superstring theory* (Cambridge University Press, UK, 1987); J. Polchinski, *String theory* (Cambridge University Press, UK, 1997).
 - [3] N. Arkani-Hamed, S. Dimopoulos, G. Dvali, *The hierarchy problem and new dimensions at a millimeter*, Phys. Lett. B **429**, 263-272 (1998); N. Arkani-Hamed, S. Dimopoulos, G. Dvali, *phenomenology, astrophysics and cosmology of theories with sub-millimeter dimensions and TeV scale quantum gravity*, Phys. Rev. D **59**, 086004 (1999).
 - [4] L. Randall and R. Sundrum, *A large mass hierarchy from a small extra dimension*, Phys. Rev. Lett. **83**, 3370 (1999).
 - [5] L. Randall and R. Sundrum, *An alternative to compactification*, Phys. Rev. Lett. **83**, 4690 (1999).
 - [6] S. Ghosh, S. Kar and H. Nandan, *Confinement of test particles in warped spacetimes*, Phys. Rev. D **82**, 024040 (2010) [arXiv:0904.2321 [gr-qc]].
 - [7] A. K. Raychaudhuri, *Relativistic cosmology. I*, Phys. Rev. **98**, 1123 (1955);
 - [8] S. W. Hawking and G. F. R. Ellis, *The large scale structure of spacetime* (Cambridge University Press, Cambridge, UK, 1973).
 - [9] R. Penrose, *Gravitational collapse and space-time singularities*, Phys. Rev. Lett. **14**, 57 (1965).
 - [10] S. W. Hawking, *Occurrence of singularities in open universes*, Phys. Rev. Lett. **15**, 689 (1965); *Singularities in the universe*, ibid **17**, 444 (1966).
 - [11] E. Poisson, *A relativists' toolkit: the mathematics of black hole mechanics* (Cambridge University Press, UK, 2004).
 - [12] R. M. Wald, *General Relativity* (University of Chicago Press, Chicago, USA, 1984).
 - [13] P. S. Joshi, *Global aspects in gravitation and cosmology* (Oxford University Press, Oxford, UK,

- 1997).
- [14] G. F. R. Ellis in *General Relativity and Cosmology, International School of Physics, Enrico Fermi—Course XLVII* (Academic Press, New York, 1971).
 - [15] I. Ciufolini and J. A. Wheeler, *Gravitation and inertia* (Princeton University Press, Princeton, USA, 1995).
 - [16] S. Kar and S. SenGupta, *The Raychaudhuri equations: a brief review*, Pramana **69**, 49 (2007); gr-qc/0611123 and references therein; S. Kar, *Introducing the Raychaudhuri equations*, Resonance, Journal of Science Education **13**, 319 (2008).
 - [17] A. Dasgupta, H. Nandan and S. Kar, *Kinematics of geodesic flows in stringy black hole backgrounds*, Phys. Rev. D **79** 124004 (2009).
 - [18] A. Dasgupta, H. Nandan and S. Kar, *Kinematics of deformable media*, Annals of Physics **323**, 1621 (2008); arXiv: 0709.0582.
 - [19] A. Dasgupta, H. Nandan and S. Kar, *Kinematics of flows on curved, deformable media*, Int. J. of Geom. Meth. Mod. Phys. **6(4)** (2009); arXiv: 0804.4089.
 - [20] R. Koley and S. Kar, *Scalar kinks and fermion localisation in warped spacetimes*, Class. Quant. Grav. **22**, 753 (2005) and references therein.
 - [21] P. Kanti, K. A. Olive and M. Pospelov, *Static solutions for brane models with a bulk scalar field*, Phys. Lett. B **481**, 386 (2000).
 - [22] V. Dzhunushaliev, V. Folomeev and M. Minamitsuji, *Thick brane solutions*, Rept. Prog. Phys. **73**, 066901 (2010) [arXiv:0904.1775 [gr-qc]].
 - [23] S. Ghosh and S. Kar, *Bulk spacetimes for cosmological braneworlds with a time-dependent extra dimension*, Phys. Rev. D **80**, 064024, (2009).
 - [24] T. C. Scott and R. B. Mann, *General Relativity and Quantum Mechanics: Towards a Generalization of the Lambert W Function*, AAEECC (Applicable Algebra in Engineering, Communication and Computing), vol. 16, no. 6, (2006) [arXiv:math-ph/0607011v2].